

Spin observables in quasi-elastic proton-nucleus scattering near 1 GeV

Richard D. Smith

Lawrence Livermore National Laboratory, University of California, Livermore, California 94550

Stephen J. Wallace

Department of Physics and Astronomy, University of Maryland, College Park, Maryland 20742

(Received 20 May 1985)

The spin dependence of quasi-elastic proton-nucleus scattering is studied using Glauber's eikonal multiple scattering theory, which is extended to include multiple knockout collisions as well as the full spin dependence of the NN amplitudes. Calculations of the cross section $d^2\sigma/d\Omega dp$ and spin observables DNN , DLL , DSS , DSL , DLS , A_y are presented and compared to data for $d^2\sigma/d\Omega dp$ and A_y from inclusive (p,p') experiments on ^{12}C at $T_{\text{lab}}=800$ MeV. The main feature seen is a drop in the spin observables in the kinematic region where two nucleon knockout dominates the cross section. As an initial study of the contribution of quasi-free Δ production to the inclusive cross section, multiple scattering theory is used to normalize a plane-wave impulse approximation calculation of $d^2\sigma/d\Omega dp$ for $p + ^{12}\text{C} \rightarrow p + \pi + ^{12}\text{C}^*$.

I. INTRODUCTION

Many aspects of high energy proton-nucleus scattering have been understood using multiple scattering theories, where the interaction with the nucleus is described as a succession of nearly free or "quasi-free" nucleon-nucleon collisions. Such a description requires that the target nucleons be weakly bound compared to the incident energy. The in-medium two-body amplitudes can then be replaced by the free on-shell NN amplitudes determined from experiment. This procedure has been successfully applied to the calculation of elastic cross sections and spin observables using Glauber theory,¹ the Kerman, McManus, and Thaler (KMT) impulse approximation,² or the more recent relativistic impulse approximation.³

The quasi-free picture of p-nucleus scattering should also work well to describe inelastic processes. Evidence of this is seen in the experimental data. A typical cross section for inclusive (p,p') scattering at $T_{\text{lab}}=800$ MeV is shown in Fig. 1 as a function of outgoing momentum at fixed laboratory scattering angle. There are three peaks in the cross section. The first is the sharp elastic peak near the beam momentum. The second is the "quasi-elastic" peak near 1300–1400 MeV/c, so called because its centroid moves in accordance with NN momentum and energy conservation. This is a signature of quasi-free elastic NN collisions where the struck nucleon is knocked into the continuum. Scattering to discrete nuclear states would appear as narrow spikes nearer the elastic peak (not shown in figure). The width of the quasi-elastic peak can be attributed to Fermi motion of struck nucleons.

At high energy quasi-elastic processes contribute only a part of the full reaction cross section, because meson production becomes possible at sufficiently high energy transfer. This is the source of the broad third peak in the cross section seen near 1000 MeV/c in Fig. 1. The dominant reaction mechanism contributing to this peak is the excitation of the $\Delta(1236)$ resonance in the projectile or tar-

get nucleons, which then either decays $\Delta \rightarrow \pi N$ or initiates a more complex reaction. Here again the centroid of the peak moves roughly in accordance with the quasi-free production of a Δ with mass ~ 300 MeV above the nucleon mass. The peak is broadened by the width of the Δ as well as by Fermi motion.

Calculations of inelastic cross sections have been carried out for both quasi-elastic⁴ and quasi-free Δ production processes⁵ using a plane wave impulse approximation (PWIA). These reproduce fairly well the positions and widths of the peaks, but the PWIA overestimates the overall magnitude and requires a phenomenological normalization. The distorted wave impulse approximation (DWIA) has also been used to calculate the quasi-elastic cross section^{4,6} and the results roughly agree with the PWIA. The main effect of the distortion is to provide the correct normalization.

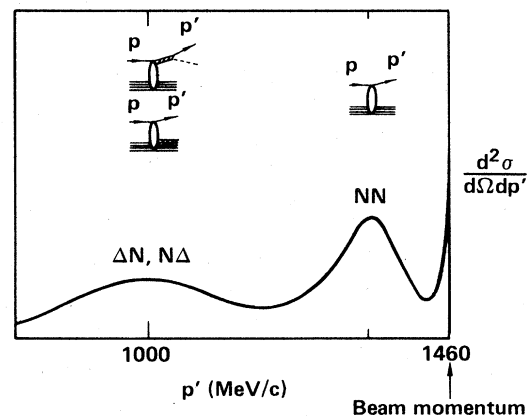


FIG. 1. Typical cross section for inclusive (p,p') scattering at $T_{\text{lab}}=800$ MeV. The quasi-elastic peak is seen near 1300–1400 MeV/c. The broad peak centered near 1000 MeV/c corresponds to Δ isobar production.

The PWIA and DWIA models include only those processes involving a single quasi-free scattering. Calculations which include multiple inelastic scattering have been carried out by Krimm, Klar, and Pirner⁷ (KKP) based on the theoretical work by Thies.⁸ They found that multiple scattering effects are not only important for normalizing the cross section, but also multiple inelastic collisions are needed in order to fill in the "dip" region between quasi-elastic and Δ production peaks. Since they used a spin-independent parametrization of the NN amplitude they were unable to calculate spin observables. But multiple inelastic collisions should also play an important role in determining spin observables in the dip region.

The main focus of this paper is a comprehensive analysis of the quasi-elastic cross section and spin observables as a function of momentum and energy transfer. Glauber's eikonal multiple scattering theory is extended to include multiple inelastic collisions as well as the full spin dependence of the NN amplitudes. In Sec. II Glauber theory is briefly reviewed. Using the formalism of a "Z-ordered product" it is extended to incorporate noncommuting interactions. The quasi-elastic cross sections and spin observables are derived in Sec. III in a form that can be evaluated numerically using a harmonic oscillator shell model and a Gaussian parametrization of the NN amplitudes. In Sec. IV the results for 800 MeV protons on ^{12}C are presented and compared to the available data on the inclusive cross section $d^2\sigma/d\Omega dp$ and A_y which were measured at the Los Alamos Meson-Physics Facility (LAMPF).^{9,10} Predictions for the remaining spin observables DNN , DSS , DLL , DLS , and DLS are also shown. These calculations contain no free parameters except for an energy shift required to bring the quasi-elastic peak in line with the data. Finally, as a preliminary investigation of the Δ region, multiple scattering theory is used to normalize the PWIA calculation of $p + A \rightarrow p + \pi + A^*$ from Ref. 5.

II. SPIN DEPENDENT MULTIPLE SCATTERING THEORY

A. Glauber series

The multiple scattering analysis of high energy p-nucleus scattering begins with the Watson series,¹¹ in which the T matrix describing transitions between initial and final nuclear status due to the scattering of a projectile is given by

$$T = \sum_{i=1}^A \tau_i + \sum_{i,j \neq i} \tau_i G \tau_j + \sum_{i,j \neq i, k \neq j} \tau_i G \tau_j G \tau_k + \dots, \quad (1a)$$

$$\tau_i = v_i + v_i G \tau_i; \quad (1b)$$

τ_i is the two-body t matrix describing a collision with the i th target nucleon. Equation (1) assumes the p-nucleus interaction can be described as a sum of two body potentials v_i . It is valid even for noncommuting interactions $[v_i, v_j] \neq 0$. The nuclear Hamiltonian H is embedded in the propagator G . If the excitation energy of intermediate states is small compared to the incident projectile energy then G may be replaced by the eikonal propagator¹² which

no longer contains H . In the center of momentum (c.m.) frame it is given by

$$G_{\text{eik}}(\mathbf{p}) = [v_{\text{lab}}(k_a - p_z + i\eta)]^{-1}, \quad (2a)$$

$$\mathbf{k}_a = k_a \hat{\mathbf{z}} = \frac{1}{2}(\mathbf{k} + \mathbf{k}'); \quad (2b)$$

v_{lab} is the laboratory velocity, and p_z is the component of \mathbf{p} along \mathbf{k}_a , the average of initial and final momenta \mathbf{k}, \mathbf{k}' . This defines a $\hat{\mathbf{z}}$ direction appropriate to the eikonal approximation, where the projectile is assumed to traverse an essentially straight line path along \mathbf{k}_a .

The Glauber multiple scattering series¹ can be derived from (1) by replacing $G \rightarrow G_{\text{eik}}$ and integrating over intermediate momenta p_z by retaining the residues of the poles in the eikonal propagators (this is known as the "eikonal pole approximation" and is discussed in Ref. 13). The coordinate dependence of the two-body amplitudes is extracted using translational invariance,

$$\langle \mathbf{p}' | \tau_i | \mathbf{p} \rangle = \exp[i(\mathbf{p} - \mathbf{p}') \cdot \mathbf{r}_i] \tau_i(\mathbf{p} - \mathbf{p}'),$$

and they are assumed to depend only on the component of momentum transfer perpendicular to $\hat{\mathbf{z}}$: $\tau_i(\mathbf{q}) \rightarrow \tau_i(\mathbf{q}_\perp)$. The resulting Glauber series is

$$\langle \mathbf{k}' | T | \mathbf{k} \rangle = -iv_{\text{lab}} \int d^2b e^{i\mathbf{q} \cdot \mathbf{b}} \Gamma(\mathbf{b}), \quad (\mathbf{q} = \mathbf{k} - \mathbf{k}'), \quad (3a)$$

$$\begin{aligned} \Gamma(\mathbf{b}) = & \sum_{i=1}^A \Gamma_i - \sum_{i,j \neq i} \Gamma_i \theta_{ij} \Gamma_j \\ & + \sum_{i,j \neq i, k \neq j} \Gamma_i \theta_{ij} \Gamma_j \theta_{jk} \Gamma_k - \dots, \end{aligned} \quad (3b)$$

$$\Gamma_i \equiv \Gamma_i(\mathbf{b} - \mathbf{b}_i), \quad \theta_{ij} \equiv \theta(z_i - z_j). \quad (3c)$$

Here $\mathbf{r}_i = (\mathbf{b}_i, z_i)$ is the coordinate for the i th target nucleon and $\theta(z)$ is the standard step function: $\theta(z) = 0$ if $z < 0$, $\theta(z) = 1$ if $z > 0$. The "profile function" Γ_i depends on the impact parameter $\mathbf{b} - \mathbf{b}_i$ of the projectile relative to the i th nucleon. It is defined in terms of the two-body amplitude τ_i by

$$\tau_i(\mathbf{q}) = -iv_{\text{lab}} \int d^2b e^{i\mathbf{q} \cdot \mathbf{b}} \Gamma_i(\mathbf{b}). \quad (4)$$

At high energy, where the binding energy of target nucleons is comparatively small, the two-body interaction is expected to resemble free nucleon-nucleon scattering, and the τ 's can be replaced by the free NN scattering amplitudes:

$$\tau(\mathbf{q}) = -\frac{2\pi}{E} f_{\text{NN}}(\mathbf{q}). \quad (5)$$

Here $E = k/v_{\text{lab}}$. Nonrelativistically $E \rightarrow \mu = mM/(m+M)$, the p-nucleus reduced mass. The NN amplitudes are accurately determined from experimental phase shifts over a wide range of energies (pp: 0 to 1000 MeV, pn: 0 to 500 MeV).¹⁴ For p-nucleus analyses f_{NN} is usually evaluated in the Breit frame¹² where it has the form

$$\begin{aligned} f_{\text{NN}}(\mathbf{q})/2ik = & A(q) + i\sigma_1 \cdot \mathbf{q} \times \hat{\mathbf{z}} C_1(q) \\ & + i\sigma_2 \cdot \mathbf{q} \times \hat{\mathbf{z}} C_2(q) + \sigma_1 \cdot \sigma_2 B(q) \\ & + \sigma_1 \cdot \mathbf{q} \sigma_2 \cdot \mathbf{q} D(q) + \sigma_1 \cdot \hat{\mathbf{z}} \sigma_2 \cdot \hat{\mathbf{z}} E(q), \end{aligned} \quad (6)$$

σ_1, σ_2 are spin operators for the incident and struck nucleons, respectively. In elastic scattering from a spin-0 nucleus only the A, C_1 terms contribute because of a trace over target spin variables. However, in quasi-elastic scattering all terms A, \dots, E contribute.

B. Z ordering

In order to deal with spin-dependent interactions, we introduce a formalism which will allow a compact representation of Γ in the noncommuting case $[\Gamma_i, \Gamma_j] \neq 0$. Define the Z-ordered product of two operators A_1, A_2 (acting in the space of target particles 1,2) as

$$Z\{A_1 A_2\} = A_1 A_2 \theta(z_1 - z_2) + A_2 A_1 \theta(z_2 - z_1). \quad (7)$$

This is exactly analogous to the "time ordered product" in quantum field theory. The Z-ordered product of n operators A_1, A_2, \dots, A_n is given by

$$Z\{A_1 \cdots A_n\} = \sum_{P_n(a)} A_{a_1} A_{a_2} \cdots A_{a_n} \theta(z_{a_1}, \dots, z_{a_n}), \quad (8)$$

where the sum is over all permutations $P_n(a) = (a_1, a_2, \dots, a_n)$ of $(1, 2, \dots, n)$, and

$$\theta(z_1, \dots, z_n) \equiv \theta(z_1 - z_2) \theta(z_2 - z_3) \cdots \theta(z_{n-1} - z_n). \quad (9)$$

Using the Z-ordered product, Γ can be written as

$$\begin{aligned} \Gamma &= \sum_{i=1}^A \Gamma_i - \sum_{i,j \neq i} \Gamma_i \theta_{ij} \Gamma_j \\ &+ \sum_{i,j \neq i, k \neq j} \Gamma_i \theta_{ij} \Gamma_j \theta_{jk} \Gamma_k - \cdots \\ &= \sum_i \Gamma_i - \sum_{i>j} Z\{\Gamma_i \Gamma_j\} + \sum_{i>j>k} Z\{\Gamma_i \Gamma_j \Gamma_k\} - \cdots \\ &= Z \left[\sum_i \Gamma_i - \sum_{i>j} \Gamma_i \Gamma_j + \sum_{i>j>k} \Gamma_i \Gamma_j \Gamma_k - \cdots \right] \\ &= 1 - Z \left[\prod_{i=1}^A (1 - \Gamma_i) \right], \quad [\Gamma_i, \Gamma_j] \neq 0. \end{aligned} \quad (10)$$

In the noncommuting case this reduces to

$$\Gamma = 1 - \prod_{i=1}^A (1 - \Gamma_i), \quad [\Gamma_i, \Gamma_j] = 0, \quad (11)$$

which is the form that appeared in Glauber's original paper.¹

To illustrate the power of this formalism, we will use it to show that unitarity of the NN interaction implies unitarity of the N-nucleus interaction. Define the eikonal S matrix for the two-body interaction by

$$s(\mathbf{b}) = 1 - \Gamma(\mathbf{b}). \quad (12)$$

Assuming the excitation energy of any states accessible through NN scattering is small compared to the incident energy, it can be shown¹⁵ that NN unitarity is expressed in the eikonal limit as

$$s^\dagger(\mathbf{b})s(\mathbf{b}) = 1. \quad (13)$$

The eikonal S matrix for N-nucleus scattering is

$$\begin{aligned} \mathbf{S}(\mathbf{b}) &= 1 - \Gamma(\mathbf{b}) \\ &= Z \left\{ \prod_{i=1}^A s_i \right\}. \end{aligned} \quad (14)$$

The unitarity of \mathbf{S} quickly follows from (13) and (14):

$$\begin{aligned} \mathbf{S}^\dagger \mathbf{S} &= \sum_{P_A(a)} \sum_{P_A(b)} s_{b_A}^\dagger \cdots s_{b_1}^\dagger s_{a_1} \cdots s_{a_A} \\ &\quad \times \theta(z_{b_1}, \dots, z_{b_A}) \theta(z_{a_1}, \dots, z_{a_A}) \\ &= \sum_{P_A(a)} s_{a_A}^\dagger \cdots s_{a_1}^\dagger s_{a_1} \cdots s_{a_A} \theta(z_{a_1}, \dots, z_{a_A}). \end{aligned}$$

In the last step the product of θ functions vanishes unless the z ordering is the same in both. Now use $s_i^\dagger s_i = 1$ [Eq. (13)] and successively eliminate all the s 's to arrive at

$$\mathbf{S}^\dagger \mathbf{S} = \sum_{P_A(a)} \theta(z_{a_1}, \dots, z_{a_A}) = 1, \quad (15)$$

which expresses N-nucleus unitarity. This result holds even when $[s_i, s_j] \neq 0$ as in the spin dependent case or in a coupled-channel multiple scattering formalism^{7,12} where s_i is a matrix connecting the various channels (such as NN and $N\Delta$).

In Ref. 15 it is shown that, in the context of this unitary eikonal multiple scattering theory, and using an independent particle model of the nucleus, the total cross section separates into elastic, quasi-elastic, and particle production contributions: $\sigma_T = \sigma_{el} + \sigma_{qe} + \sigma_{\pi}$. This provides a unified picture of the high energy p-nucleus reaction. The unitarity ensures that all the reactive content is accounted for and that each piece of the total cross section is properly normalized. In the next section the quasi-elastic contribution will be analyzed in detail.

III. QUASI-ELASTIC SCATTERING

A. Cross section

The cross section due to quasi-elastic scattering has the form

$$d\sigma_{qe} \sim \int d^2b d^2b' e^{iq \cdot (b-b')} \langle 0 | \Gamma^\dagger(\mathbf{b}') \hat{Q} \Gamma(\mathbf{b}) | 0 \rangle, \quad (16)$$

where $|0\rangle$ represents the nuclear ground state, and

$$\hat{Q} = \sum_{\alpha \neq 0} |\alpha\rangle \langle \alpha|$$

projects onto nuclear excited states. Using $\hat{Q} = 1 - |0\rangle \langle 0|$, we have

$$\begin{aligned} \langle 0 | \Gamma^\dagger \hat{Q} \Gamma | 0 \rangle &= \langle 0 | \mathbf{S}^\dagger \hat{Q} \mathbf{S} | 0 \rangle \\ &= \langle 0 | \mathbf{S}^\dagger \mathbf{S} | 0 \rangle - \langle 0 | \mathbf{S}^\dagger | 0 \rangle \langle 0 | \mathbf{S} | 0 \rangle. \end{aligned} \quad (17)$$

(For brevity the \mathbf{b}, \mathbf{b}' dependence of Γ, Γ^\dagger is omitted. Henceforth $\Gamma^\dagger, \mathbf{S}^\dagger, \Gamma_i^\dagger$, and s_i^\dagger implicitly depend on \mathbf{b}' , and $\Gamma, \mathbf{S}, \Gamma_i$, and s_i depend on \mathbf{b} .) Consider the ground state matrix elements in (17). In the independent particle model the ground state wave function is

$$\langle \mathbf{r}_1, \dots, \mathbf{r}_A | 0 \rangle = \Psi_0(\mathbf{r}_1, \dots, \mathbf{r}_A) = \prod_{i=1}^A \phi_i(\mathbf{r}_i). \quad (18)$$

Assume for the moment that the single particle densities

$$\begin{aligned} \langle 0 | \mathbf{S}^\dagger \mathbf{S} | 0 \rangle &= \sum_{p_A(a)} \langle 0 | s_{a_A}^\dagger \cdots s_{a_1}^\dagger s_{a_1} \cdots s_{a_A} \theta(z_{a_1}, \dots, z_{a_A}) | 0 \rangle \\ &= A! \langle 0 | s_A^\dagger \cdots s_1^\dagger s_1 \cdots s_A \theta(z_1, \dots, z_A) | 0 \rangle, \end{aligned} \quad (19a)$$

$$\langle 0 | \mathbf{S} | 0 \rangle = A! \langle 0 | s_1 \cdots s_A \theta(z_1, \dots, z_A) | 0 \rangle. \quad (19b)$$

It would be nice to be rid of the θ functions which complicate z integrals in the ground state matrix elements. In an integral of the form

$$I[F] = \int \prod_{i=1}^A [dz_i] F(z_1, \dots, z_A) \theta(z_1, \dots, z_A)$$

if F is symmetric under $z_i \leftrightarrow z_j$, then since the z_i 's are dummy variables, $\theta(z_1, \dots, z_A)$ may be replaced with any permuted ordering $\theta(z_{a_1}, \dots, z_{a_A})$. Hence it may be replaced by

$$\theta(z_1, \dots, z_A) \rightarrow \frac{1}{A!} \sum_{p_A(a)} \theta(z_{a_1}, \dots, z_{a_A}) = \frac{1}{A!}. \quad (20)$$

In the noncommuting case $[s_i, s_j] \neq 0$ the z integrands in Eqs. (19a) and (19b) are not symmetric unless the ground state happens to be symmetric under $z_i \leftrightarrow z_j$ [this would be true if, for example, the single particle density is a Gaussian:

$$\rho(r_i) \sim e^{-ar_i^2},$$

or if the nucleus is a deuteron, since its density depends only on $(\mathbf{r}_1 - \mathbf{r}_2)^2$]. Nevertheless, we will make the replacement $\theta(z_1, \dots, z_A) \rightarrow 1/A!$ in the matrix elements (19) as an approximation:

$$\langle 0 | \mathbf{S}^\dagger \mathbf{S} | 0 \rangle \cong \langle 0 | s_A^\dagger \cdots s_1^\dagger s_1 \cdots s_A | 0 \rangle, \quad (21a)$$

$$\langle 0 | \mathbf{S} | 0 \rangle \cong \langle 0 | s_1 \cdots s_A | 0 \rangle. \quad (21b)$$

The first-order correction to this approximation is a double scattering term which vanishes in the independent particle model. This can be seen by considering the z integral for the double scattering contribution to (19a) or (19b). It involves

$$\int dz_1 dz_2 \rho(r_1) \rho(r_2) \theta(z_1 - z_2) = \frac{1}{2!} \int dz_1 dz_2 \rho(r_1) \rho(r_2). \quad (22)$$

This equality holds because ρ depends only on $r_i = |\mathbf{r}_i|$. Thus the replacement $\theta(z_1 - z_2) \rightarrow 1/2!$ can be made in the double scattering contribution regardless of the form of $\rho(r_i)$. The lowest order nonvanishing correction to (21) is a triple scattering term involving Γ_i or Γ_i^\dagger or both for three distinct nucleons. Inserting (21) into (17) we have

$$\langle 0 | \Gamma^\dagger \hat{Q} \Gamma | 0 \rangle \cong \langle 0 | s_A^\dagger \cdots s_1^\dagger \hat{Q} s_1 \cdots s_A | 0 \rangle. \quad (23)$$

$\rho_i(r_i) = |\phi_i(r_i)|^2$ are all the same: $\rho_i(r_i) = \rho(r_i)$, and that the s_i 's are the same for pp and pn scattering: $s_i(\mathbf{b} - \mathbf{b}_i) = s(\mathbf{b} - \mathbf{b}_i)$ (in practice suitable averages will be taken). We then have

In the independent particle model \hat{Q} can be expressed in terms of the single particle projection operators:

$$p_i^0 = |\phi_i\rangle \langle \phi_i|, \quad p_i^* = \sum_{\alpha_i} |\alpha_i\rangle \langle \alpha_i|; \quad (24)$$

$|\phi_i\rangle$ is the single particle ground state for the i th nucleon, and $|\alpha_i\rangle$ is a single particle excited state. Since $p_i^0 + p_i^* = 1$, \hat{Q} can be written as

$$\begin{aligned} \hat{Q} &= \prod_{i=1}^A (p_i^0 + p_i^*) - \sum_{i=1}^A p_i^0 \\ &= \sum_{i=1}^A p_i^* \prod_{j \neq i} p_j^0 + \sum_{i > j} p_i^* p_j^* \prod_{k \neq i, j} p_k^0 \\ &\quad + \cdots + \prod_{i=1}^A p_i^* \\ &= \hat{Q}^{(1)} + \hat{Q}^{(2)} + \cdots + \hat{Q}^{(A)}. \end{aligned} \quad (25)$$

Thus $\hat{Q}^{(n)}$ projects onto states where n nucleons have been excited out of the ground state by quasi-free or "hard" collisions with the projectile. The contribution to the cross section from single hard scattering processes involves

$$\begin{aligned} \langle 0 | \Gamma^\dagger \hat{Q}^{(1)} \Gamma | 0 \rangle \\ = \langle 0 | s_A^\dagger \cdots s_1^\dagger \left[\sum_{i=1}^A p_i^* \prod_{j \neq i} p_j^0 \right] s_1 \cdots s_A | 0 \rangle. \end{aligned} \quad (26)$$

Expressed in terms of the single particle matrix elements

$$\begin{aligned} \Omega &= \langle \phi_i | s(\mathbf{b} - \mathbf{b}_i) | \phi_i \rangle, \\ \Omega^\dagger &= \langle \phi_i | s^\dagger(\mathbf{b}' - \mathbf{b}_i) | \phi_i \rangle, \\ \gamma_\alpha &= \langle \alpha_i | s(\mathbf{b} - \mathbf{b}_i) | \phi_i \rangle = -\langle \alpha_i | \Gamma(\mathbf{b} - \mathbf{b}_i) | \phi_i \rangle, \\ \gamma_\alpha^\dagger &= \langle \phi_i | s^\dagger(\mathbf{b}' - \mathbf{b}_i) | \alpha_i \rangle, \end{aligned} \quad (27)$$

Eq. (26) becomes

$$\langle 0 | \Gamma^\dagger \hat{Q}^{(1)} \Gamma | 0 \rangle = \sum_{\alpha} \sum_{(m+n=A-1)} \Omega_m^\dagger \gamma_\alpha^\dagger \Omega_n^\dagger \Omega_n \gamma_\alpha \Omega_m, \quad (28)$$

where $\Omega_m \equiv (\Omega)^m$, and $\sum_{(m+n=A-1)}$ means sum over all m, n such that $m+n=A-1$. This equation has a simple physical interpretation: $\Omega_m, \Omega_m^\dagger$ describe the distortion due to the interaction with $m \leq A-1$ nucleons before the hard collision, and $\Omega_n, \Omega_n^\dagger$ describe the final state distortion due to interaction with the remaining $n=A-1-m$ nucleons after the hard collision. This is analogous to the

DWIA if the distorted waves are generated by solving the Schrödinger equation with an optical potential

$$u_0 = \left\langle 0 \left| \sum_{i=1}^A \tau_i \right| 0 \right\rangle$$

describing the elastic scattering.

The contribution from n hard scatterings is

$$\langle 0 | \Gamma^\dagger \hat{Q}^{(n)} \Gamma | 0 \rangle = \sum_{\alpha_1, \dots, \alpha_n} \sum_{(m_0+m_1+\dots+m_n=A-n)} \Omega_{m_0}^\dagger \gamma_{\alpha_1}^\dagger \Omega_{m_1}^\dagger \dots \gamma_{\alpha_n}^\dagger \Omega_{m_n}^\dagger \Omega_{m_n} \gamma_{\alpha_n} \dots \Omega_{m_1} \gamma_{\alpha_1} \Omega_{m_0}. \quad (29)$$

Here α_n labels the final state for the n th excited particle. The spin structure in Eq. (29) is complicated and difficult to work with in practical calculations of spin-dependent quasi-elastic cross sections. To simplify it we will assume the distortion factors Ω are spin independent, involving only the A term in the NN amplitude (6). Then Eq. (29), summed over n , becomes

$$\langle 0 | \Gamma^\dagger \hat{Q} \Gamma | 0 \rangle = \sum_{n=1}^A \binom{A}{n} (\Omega^\dagger \Omega)^{A-n} \sum_{\alpha_1, \dots, \alpha_n} \gamma_{\alpha_1}^\dagger \dots \gamma_{\alpha_n}^\dagger \gamma_{\alpha_n} \dots \gamma_{\alpha_1}; \quad (30)$$

$(\Omega^\dagger \Omega)^{A-n}$ is the scalar distortion. To test this approximation the single scattering contribution will later be calculated with the full spin dependent Ω using (28), and compared to the $n=1$ term in (30). We will find that the distortion, whether scalar or spin dependent, serves mainly to normalize the cross sections. The spin observables, which are ratios of spin-dependent to spin-averaged cross sections, are largely unaffected by it. Therefore Eq. (30) turns out to be a good approximation to (29).

At high energy, the quasi-elastic cross section is dominated by knockout processes. The knockout states will be described by plane waves of momentum \mathbf{k}_i and energy $k_i^2/2m$:

$$\sum_{\alpha_1, \dots, \alpha_n} \prod_{i=1}^n |\alpha_i\rangle \langle \alpha_i| \rightarrow \int \prod_{i=1}^n \left[\frac{d^3 k_i}{(2\pi)^3} |\mathbf{k}_i\rangle \langle \mathbf{k}_i| \right] \delta \left[\omega - \sum_{i=1}^n \epsilon(k_i) \right], \quad (31)$$

$$\omega = E_k - E_p, \quad E_p = \sqrt{p^2 + m^2}, \quad \epsilon(k_i) = \epsilon_B + k_i^2/2m.$$

Here $|\mathbf{k}_i\rangle$ is a plane wave state:

$$\langle \mathbf{r}_i | \mathbf{k}_i \rangle = e^{i\mathbf{k}_i \cdot \mathbf{r}_i}.$$

ω is the energy lost by the projectile (which has initial and final momenta \mathbf{k}, \mathbf{p}), and $\epsilon(k_i)$ is the energy lost on the i th hard collision. ϵ_B is the average (positive) binding energy per nucleon. There is, by definition, energy loss only on the hard collisions, although momentum may be transferred on any two-body collision. Contributions to the energy loss as well as corrections to the scattering amplitude due to target recoil are neglected for a heavy nucleus. Under these conditions the double differential cross section is given by

$$\frac{d^2 \sigma_{qe}}{d\Omega dp} = \frac{v_{lab} p^2}{(2\pi)^2} \int d^2 b d^2 b' e^{i\mathbf{q} \cdot (\mathbf{b} - \mathbf{b}')} \sum_{n=1}^A \binom{A}{n} (\Omega^\dagger \Omega)^{A-n} \int \prod_{i=1}^n \left[\frac{d^3 k_i}{(2\pi)^3} \right] \delta \left[\omega - \sum_{i=1}^n \epsilon(k_i) \right] \times \text{tr}(\text{target}) \{ \gamma_n^\dagger \gamma_{n-1}^\dagger \dots \gamma_1^\dagger \gamma_1 \dots \gamma_{n-1} \gamma_n \}, \quad (32a)$$

$$\gamma_i^\dagger = \langle \mathbf{k}_i | \Gamma(\mathbf{b} - \mathbf{b}_i) | \phi_i \rangle,$$

$$\gamma_i = \langle \phi_i | \Gamma^\dagger(\mathbf{b}' - \mathbf{b}_i) | \mathbf{k}_i \rangle. \quad (32b)$$

The trace is over target spin variables and assumes a spin-0 nucleus. [We use a normalized trace throughout: $\text{tr}(\boldsymbol{\pi} \cdot \boldsymbol{\sigma}) = 0$, $\text{tr}(1) \equiv 1$.]

B. Spin observables

The polarization asymmetry A_y and the polarization transfer observables DNN , DSS , DLL , DLS , and DSL (sometimes called the "triple scattering parameters") form a complete set of spin observables for p-nucleus scattering consistent with parity conservation. These are linear combinations of another complete set, the D_{ij} 's, which in the present analysis are given by

$$D_{ij}(q_{\perp}, \omega) = S_{ij}(q_{\perp}, \omega) / S_{00}(q_{\perp}, \omega) \quad (i, j = 0, 1, 2, 3), \quad (33a)$$

$$S_{ij}(q_{\perp}, \omega) = \int d^2b d^2b' e^{iq \cdot (b-b')} \sum_{n=1}^A \binom{A}{n} (\Omega^\dagger \Omega)^{A-n} \int \prod_{i=1}^n \left[\frac{d^3k_i}{(2\pi)^3} \right] \delta \left[\omega - \sum_{i=1}^n \epsilon(k_i) \right] \text{tr} \{ \sigma_i (\gamma_n^\dagger \cdots \gamma_1^\dagger) \sigma_j (\gamma_1 \cdots \gamma_n) \}. \quad (33b)$$

Here the trace is in the projectile spin space (a trace over target spin variables is implied) which is spanned by the basis

$$\sigma_0 = 1, \quad \sigma_1 = \sigma \cdot \hat{n}, \quad \sigma_2 = \sigma \cdot \hat{q}_{\perp}, \quad \sigma_3 = \sigma \cdot \hat{z}, \quad (34)$$

$$\hat{n} = \mathbf{k} \times \mathbf{k}' / |\mathbf{k} \times \mathbf{k}'|, \quad \hat{z} = (\mathbf{k} + \mathbf{k}') / |\mathbf{k} + \mathbf{k}'|, \quad \hat{q}_{\perp} = \hat{z} \times \hat{n}.$$

This basis is defined using $\hat{z} = \hat{k}_z$ and \hat{q}_{\perp} which is appropriate to the eikonal approximation. It should be noted that the D_{ij} 's are usually defined with respect to $\hat{q} = (\mathbf{k} - \mathbf{k}') / |\mathbf{k} - \mathbf{k}'|$ and $\hat{p} = \hat{q} \times \hat{n}$ in place of $\hat{q}_{\perp}, -\hat{z}$.¹⁶

For parity conserving interactions the D_{ij} 's form a block diagonal matrix:

$$D = \begin{pmatrix} 1 & D_{01} & & 0 \\ D_{10} & D_{11} & & \\ & & D_{22} & D_{23} \\ 0 & & & D_{32} & D_{33} \end{pmatrix}. \quad (35)$$

In spin- $\frac{1}{2}$ -spin-0 scattering $D_{10} = D_{01}$ (i.e., the asymmetry $A_y = P$ the polarization) and $D_{32} = -D_{23}$. Thus there are five independent D_{ij} 's which together with the cross section comprise a complete set of observables for inclusive (p,p') scattering on spin-0 nuclei.

The quantities normally measured in laboratory experiments have spin states referred to the incident and final (primed) momentum directions: $L = \mathbf{k}/k$, $L' = \mathbf{k}'/k'$, $N = N' = \hat{n}$, and $S = N \times L$, $S' = N' \times L'$. The laboratory observables are

$$\frac{d^2\sigma}{d\Omega dp} = \frac{v_{\text{lab}} p^2}{(2\pi)^2} S_{00}, \quad (36a)$$

$$A_y = D_{01} = D_{10}, \quad (36b)$$

$$DLL = D_{qq} \cos(\theta + \theta_q) \cos\theta_q + D_{zz} \sin(\theta + \theta_q) \sin\theta_q + D_{qz} \sin\theta, \quad (36c)$$

$$DSS = D_{qq} \sin(\theta + \theta_q) \sin\theta_q + D_{zz} \cos(\theta + \theta_q) \cos\theta_q + D_{qz} \sin\theta, \quad (36d)$$

$$DSL = -D_{qq} \cos(\theta + \theta_q) \sin\theta_q + D_{zz} \sin(\theta + \theta_q) \cos\theta_q - D_{qz} \cos\theta, \quad (36e)$$

$$DLS = -D_{qq} \sin(\theta + \theta_q) \cos\theta_q + D_{zz} \cos(\theta + \theta_q) \sin\theta_q + D_{qz} \cos\theta, \quad (36f)$$

$$DNN = D_{nn}. \quad (36g)$$

Here we have written D_{qq}, D_{qz} in place of D_{22}, E_{23} , etc., and primes have been omitted from final laboratory direc-

tions (e.g., $DLL' \rightarrow DLL$). θ is the laboratory scattering angle, and θ_q is the angle between \mathbf{k} and \mathbf{q}_{\perp} ($\cos\theta_q = \hat{k} \cdot \hat{q}_{\perp}$). [Formulae similar to 36(c)-(g) also appear in Eq. (7) of Ref. 16 with the D_{ij} 's defined using the basis $\hat{n}, \hat{q}, \hat{p}$. However, they contain two typographical errors: in the equation for DSS' the term $+D_{qp} \sin\theta$ should be replaced with $-D_{qp} \sin\theta$, and in the equation for DSL' the term $D_{pp} \sin(\theta + \theta_q) \cos\theta_q + D_{qp} \cos\theta$ should be replaced with $D_{pp} \sin(\theta + \theta_q) \cos\theta_q + D_{qp} \cos\theta$. Here θ_q refers to the angle between \mathbf{k} and \mathbf{q} rather than \mathbf{k} and \mathbf{q}_{\perp} as in our notation.]

C. NN amplitudes and the nuclear ground state

To simplify the evaluation of (32) and (33), the terms A, \dots, E in the NN amplitudes (6) will be approximated as Gaussians:

$$A(q) = A_0 e^{-\eta_A q^2},$$

etc., with parameters fit to the Breit frame amplitudes determined from experiment.¹⁴ This procedure is often used in Glauber theory.¹⁷ It is reasonably accurate and is discussed in more detail in Refs. 12 and 15. The Gaussian parameters for $T_{\text{lab}} = 800$ MeV in the Breit frame of a heavy nucleus ($M \gg m$) are given in Table I.

Since the multiple scattering formalism developed here does not specifically take into account the difference between protons and neutrons in the target, the pp, pn amplitudes are averaged as follows. In elastic collisions, which contribute to the distortion, the pn, pn amplitudes can interfere, so the Gaussian parameters are taken to be the average of the pp, pn values. However, in a hard collision the knocked-out nucleon is either p or n, and these processes do not interfere. Therefore at each stage in a sequence of knockouts the contributions from pp, pn collisions are computed independently and then averaged.

Calculations will be performed for ^{12}C at $T_{\text{lab}} = 800$ MeV. Single particle matrix elements are evaluated using harmonic oscillator shell model wave functions for the s and p shells:

$$\begin{aligned} \phi_0(\mathbf{r}) &= \left[\frac{\alpha}{\pi} \right]^{3/4} e^{-\alpha r^2/2}, \\ \phi_{1m}(\mathbf{r}) &= \left[\frac{\alpha}{\pi} \right]^{3/4} (2\alpha)^{1/2} r_m e^{-\alpha r^2/2}, \\ r_m &= \begin{cases} \mp (r_1 \pm i r_2) / \sqrt{2} \\ r_3 \end{cases} \end{aligned} \quad (37)$$

The single particle density, which is used in evaluating Ω , is taken to be a weighted average:

TABLE I. 800 MeV parameters for Gaussian NN amplitudes. (Parameters are for the Breit frame in a heavy nucleus: $A \rightarrow \infty$.)

	A_0 (GeV ⁻²)	B_0 (GeV ⁻²)	C_{10} (GeV ⁻³)	C_{20} (GeV ⁻³)	D_0 (GeV ⁻⁴)	E_0 (GeV ⁻²)
PP	4.80 + i0.06	-0.18 + i1.11	-1.24 - i5.33	-2.69 - i5.03	-9.1 - i122.0	1.09 - i0.43
PN	3.95 + i1.28	-0.21 - i1.41	-1.97 - i4.19	-3.18 - i4.97	-4.35 + i1.33	0.09 + i0.67
	η_A (GeV/c) ⁻²	η_B	η_{C_1}	η_{C_2}	η_D	η_E
PP	4.18 - i3.01	12.07 + i14.26	3.42 + i1.24	2.54 + i0.02	24.5 + i5.9	20.2 - i9.12
PN	4.45 - i2.28	2.44 - i1.66	3.87 + i0.48	3.75 - i0.25	20.6 - i1.26	0.61 - i7.4

$$\rho(r) = \frac{1}{3} |\phi_0|^2 + \frac{2}{3} \left[\frac{1}{3} \sum_m |\phi_{1m}|^2 \right]$$

$$= \frac{1}{3} \left[\frac{\alpha}{\pi} \right]^{3/2} e^{-ar^2(1 + \frac{4}{3}ar^2)}. \quad (38)$$

The oscillator parameter α is determined from the nuclear rms radius: $\alpha = \frac{13}{6} \langle r^2 \rangle$ by taking $\langle r^2 \rangle^{1/2} = 2.5$ fm for ¹²C. Contributions from knockout collisions involve the Wigner transform of the single particle density $\rho_W(r, p)$

which is similarly averaged over shells. The binding energy ϵ_B [Eq. (31)] is determined from electron scattering. Averaging the proton and neutron binding energies for the *s* and *p* shells taken from Ref. 18, we have $\epsilon_B = 25.72$ MeV.

D. Evaluation of S_{ij}

We return to Eq. (33) for S_{ij} . The central part describing the sequence of inelastic collisions can be separated by writing

$$S_{ij}(q_1, \omega) = \int d^2b d^2b' e^{iq \cdot (b-b')} \sum_{n=1}^A \binom{A}{n} [\Omega^*(b') \Omega(b)]^{A-n} W_{ij}^{(n)}(b', b, \omega), \quad (39a)$$

$$W_{ij}^{(n)}(b', b, \omega) = \int \prod_{i=1}^n \left[\frac{d^3k_i}{(2\pi)^3} \right] \delta \left[\omega - \sum_i \epsilon_i \right] \text{tr} \{ \sigma_i (\hat{\gamma}_n^\dagger \cdots \hat{\gamma}_1^\dagger) \sigma_j (\hat{\gamma}_1 \cdots \hat{\gamma}_n) \}. \quad (39b)$$

Henceforth all operators in the projectile spin space expect the basis matrices σ_i [Eq. (34)] will be denoted by carets:

$$\hat{A} = \sum_{i=0}^3 A_i \sigma_i.$$

The integrals d^3k_i over final momenta of the unobserved nucleons are complicated by the presence of the energy conserving delta function which depends on all the k_i . Following KKP, we overcome this problem by Fourier transforming $W_{ij}^{(n)}$ with respect to ω :

$$W_{ij}^{(n)}(b', b, \omega) = \int \frac{dt}{2\pi} e^{i\omega t} \tilde{W}_{ij}^{(n)}(b', b, t), \quad (40a)$$

$$\tilde{W}_{ij}^{(n)}(b', b, t) = \int \prod_{i=1}^n \left[\frac{d^3k_i}{(2\pi)^3} e^{-i\epsilon_i t} \right] \text{tr} \{ \cdots \}. \quad (40b)$$

We now proceed to evaluate $\tilde{W}_{ij}^{(n)}$ analytically. Define $\hat{U}_j^{(n)}$ by

$$\tilde{W}_{ij}^{(n)}(b', b, t) = \text{tr} [\sigma_i \hat{U}_j^{(n)}(b', b, t)], \quad (41a)$$

$$\hat{U}_j^{(n)} = \int \prod_{i=1}^n \left[\frac{d^3k_i}{(2\pi)^3} e^{-i\epsilon_i t} \right] \hat{\gamma}_n^\dagger \cdots \hat{\gamma}_1^\dagger \sigma_j \hat{\gamma}_1 \cdots \hat{\gamma}_n$$

$$= \int \frac{d^3k_n}{(2\pi)^3} e^{-i\epsilon_n t} \hat{\gamma}_n^\dagger \hat{U}_j^{(n-1)} \hat{\gamma}_n. \quad (41b)$$

Now reexpress $\hat{\gamma}_n$ in terms of $\hat{f} \equiv f_{NN}/ik$:

$$\hat{\gamma}_n = \langle \mathbf{k}_n | \hat{\Gamma}(\mathbf{b} - \mathbf{b}_n) | \phi_n \rangle$$

$$= \int d^3r_n e^{-i\mathbf{k}_n \cdot \mathbf{r}_n} \phi(\mathbf{r}_n)$$

$$\times \frac{1}{2\pi} \int d^2q e^{-iq \cdot (\mathbf{b} - \mathbf{b}_n)} \hat{f}(q). \quad (42)$$

After some manipulations involving a change of variables to

$$\mathbf{R} = \frac{1}{2}(\mathbf{r}_n + \mathbf{r}'_n), \quad \mathbf{x} = \mathbf{r}_n - \mathbf{r}'_n,$$

$$\mathbf{Q} = \frac{1}{2}(\mathbf{q} + \mathbf{q}'), \quad \boldsymbol{\epsilon} = \mathbf{q} - \mathbf{q}', \quad (43)$$

$$\mathbf{B} = \frac{1}{2}(\mathbf{b} + \mathbf{b}'), \quad \boldsymbol{\beta} = \mathbf{b} - \mathbf{b}',$$

and the replacement

$$\int \frac{d^2\epsilon}{(2\pi)^2} \epsilon^{-i\epsilon \cdot (\mathbf{B} - \mathbf{R}_1)} F(\boldsymbol{\epsilon}, \mathbf{R}_1) \rightarrow \delta^2(\mathbf{B} - \mathbf{R}_1) F(i\nabla_B, \mathbf{B}),$$

we find

$$\hat{U}_j^{(n)} = \int d^2Q e^{-iQ \cdot \boldsymbol{\beta}} \hat{f}^\dagger(Q - i\nabla_B/2)$$

$$\times \hat{U}_j^{(n-1)} \hat{f}(Q + i\nabla_B/2) R(B, Q, t), \quad (44a)$$

$$R(B, Q, t) = \int d^3k_n e^{-i\epsilon(k_n)t} \tilde{\rho}_w(B, |\mathbf{k}_n - \mathbf{Q}|), \quad (44b)$$

$$\tilde{\rho}_w(B,p) = \int dz \rho_w(R,p), \quad \mathbf{R} = (\mathbf{B}, z), \quad (44c)$$

$$\begin{aligned} \rho_w(R,p) &= \int \frac{d^3x}{(2\pi)^3} e^{-i\mathbf{p}\cdot\mathbf{x}} \phi_n^*(\mathbf{R}-\mathbf{x}/2) \phi_n(\mathbf{R}+\mathbf{x}/2), \\ &\rightarrow \int \frac{d^3x}{(2\pi)^3} e^{-i\mathbf{p}\cdot\mathbf{x}} \sum_{\lambda} a_{\lambda} \phi_{\lambda}^*(\mathbf{R}-\mathbf{x}/2) \phi_{\lambda}(\mathbf{R}+\mathbf{x}/2). \end{aligned} \quad (44d)$$

The ∇_B 's act only on $R(B, Q, t)$ not on $\hat{U}_j^{(n-1)}$. $\rho_w(r, p)$ is the Wigner transform of the single particle density, and $\sum_{\lambda} a_{\lambda}$ represents the weighted average over shells.

Before proceeding, consider the physical content of Eq. (44). The Wigner transform $\tilde{\rho}_w(B, p)$ is associated with the probability of finding a target nucleon at the classical impact parameter B with momentum $p = |\mathbf{k}_n - \mathbf{Q}|$. Thus the scattering can be viewed classically as a sequence of collisions in phase space (see Ref. 8). The function $R(B, Q, t)$ contains all the nuclear structure information and is independent of the NN amplitudes. It is related to the single particle nuclear response function $R_1(Q, \omega)$ by

$$\begin{aligned} R_1(Q, \omega) &= \int d^3k n(\mathbf{k} - \mathbf{Q}) \delta(\omega - \epsilon_B - k^2/2m) \\ &= \int \frac{dt}{2\pi} e^{-i\omega t} \int d^2B R(B, Q, t), \end{aligned} \quad (45)$$

where $n(\mathbf{p})$ is the single particle density in momentum space. The essential nuclear information contained in R_1 is the position of the single knockout peak, given roughly by $\omega_0 = \epsilon_B + Q^2/2m$, and its width due to the momentum distribution (Fermi motion) of struck nucleons. This width is determined by the oscillator parameter α .

We now wish to approximate

$$\begin{aligned} \hat{f}^\dagger(\mathbf{Q} - i\nabla_B/2) \hat{U} \hat{f}(\mathbf{Q} + i\nabla_B/2) \tilde{\rho}_w(B, |\mathbf{k} - \mathbf{Q}|) \\ \rightarrow \hat{f}^\dagger(\mathbf{Q}) \hat{U} \hat{f}(\mathbf{Q}) \tilde{\rho}_w(B, |\mathbf{k} - \mathbf{Q}|). \end{aligned} \quad (46)$$

This approximation was also made by KKP in the spin-independent case. Consider the structure of \hat{f} :

$$\frac{1}{2} \hat{f}(\mathbf{q}) = A(\mathbf{q}) + i\sigma_i \cdot \mathbf{q} \times \hat{\mathbf{z}} C_1(\mathbf{q}) + \dots$$

Terms dropped by replacing $A(\mathbf{Q} + i\nabla_B/2) \rightarrow A(\mathbf{Q})$, $C_1(\mathbf{Q} + i\nabla_B/2) \rightarrow C_1(\mathbf{Q})$, etc., vanish in the short range approximation $(R_{NN}/R_{nuc})^2 \rightarrow 0$ (where $R_{NN} \sim \eta_A^{1/2} \sim \eta_c^{1/2}$ is the range of the NN force, and $R_{nuc} \sim \alpha^{-1/2}$ is the nuclear radius). Thus

$$S_{ij}(q_1, \omega) = \sum_{n=1}^A \binom{A}{n} \int d^2\beta e^{i\mathbf{q}\cdot\beta} \int d^2B [\Omega^*(b') \Omega(b)]^{A-n} \int_{-\infty}^{\infty} dt e^{-i\omega t} \tilde{W}_{ij}^{(n)}(\beta, B, t). \quad (51)$$

(In the distortion $b' = |\mathbf{B} - \frac{1}{2}\beta|$, $b = |\mathbf{B} + \frac{1}{2}\beta|$.) $\tilde{W}_{ij}^{(n)}$ depends on B, β and powers of $\hat{\mathbf{q}}_1 \cdot \hat{\beta}$, so integrals over the azimuthal angle in $\int d^2\beta$ can be evaluated analytically in terms of the cylindrical Bessel functions $J_m(q_1\beta)$. Reference 15 contains a detailed discussion of the numerical integrations.

$$\begin{aligned} \frac{1}{2} \hat{f}(\mathbf{Q} + i\nabla_B/2) \\ \rightarrow A(\mathbf{Q}) + i\sigma_1 \cdot (\mathbf{Q} + i\nabla_B/2) \times \hat{\mathbf{z}} C_1(\mathbf{Q}) + \dots \end{aligned} \quad (47)$$

(short range approximation). To arrive at (46) we must go one step further and eliminate all terms involving $\nabla_B \rho_w$. This is consistent with the approximation of scalar distortion, which amounts to dropping terms containing $\nabla_B \rho$. In a spin-0 nucleus Ω has the form:

$$\begin{aligned} \Omega(\mathbf{b}) &= 1 - \int d^3r_i [\Gamma_A(\mathbf{b} - \mathbf{b}_i) \\ &\quad - \Gamma_c(\mathbf{b} - \mathbf{b}_i) \sigma_1 \cdot \nabla_{b_i} \times \hat{\mathbf{z}}] \rho(r_i), \end{aligned} \quad (48a)$$

$$\Gamma_A(b) = \frac{1}{\pi} \int d^2q e^{-i\mathbf{q}\cdot\mathbf{b}} A(\mathbf{q}), \quad (48b)$$

$$\Gamma_c(b) = \frac{1}{\pi} \int d^2q e^{-i\mathbf{q}\cdot\mathbf{b}} C_1(\mathbf{q}).$$

Thus if the $\nabla_b \rho$ term is dropped, Ω becomes spin independent, involving only the A term in f_{NN} . One might expect the $\nabla \rho$ terms to be important, because most of the scattering takes place near the surface where $\nabla \rho \neq 0$ (this is due to the distortion, which cuts down the cross section if the projectile passes through much of the nuclear interior). Also, in elastic scattering the spin observables vanish when the $\nabla \rho$ terms are dropped. However, in the inelastic case they turn out to be relatively unimportant. This will be seen by comparing the single knockout Ay with and without all $\nabla \rho$, $\nabla \rho_w$ terms.

Inserting (46) into (44) we have

$$\begin{aligned} \hat{U}_j^{(n)}(\beta, B, t) &= \int d^2Q e^{-i\mathbf{Q}\cdot\beta} \hat{f}^\dagger(\mathbf{Q}) \\ &\quad \times \hat{U}_j^{(n-1)} \hat{f}(\mathbf{Q}) R(B, Q, t), \end{aligned} \quad (49a)$$

$$\begin{aligned} \hat{U}_j^{(1)}(\beta, B, t) &= \int d^2Q e^{-i\mathbf{Q}\cdot\beta} \hat{f}^\dagger(\mathbf{Q}) \\ &\quad \times \sigma_j \hat{f}(\mathbf{Q}) R(B, Q, t). \end{aligned} \quad (49b)$$

Using the wave functions (37) R can be shown to have the form:

$$R(B, Q, t) = e^{-\eta(t)Q^2} [g(B, t) + Q^2 h(B, t)]. \quad (50)$$

With the Gaussian parametrization of $\hat{f}(\mathbf{Q})$, Eq. (49) can be evaluated analytically. Expressions for $R(B, Q, t)$ and the components of $\hat{U}_j^{(1)}$ are given in Ref. 15. Equations (49) define an iterative procedure for determining $\hat{U}_j^{(n)}$ and hence $\tilde{W}_{ij}^{(n)}$ [Eq. 41(a)]. $\tilde{W}_{ij}^{(n)}$ is calculated with one numerical Fourier transform in the t variable [Eq. (40a)]. Once this is known, S_{ij} is found by numerically integrating over the magnitudes of $\beta = |\beta|$, $B = |B|$:

IV. RESULTS AND DISCUSSION

A. Quasi-elastic cross sections

Theoretical curves for the cross section at $\theta = 15^\circ$ based on Eqs. (51) and (36a) are shown as a function of outgoing

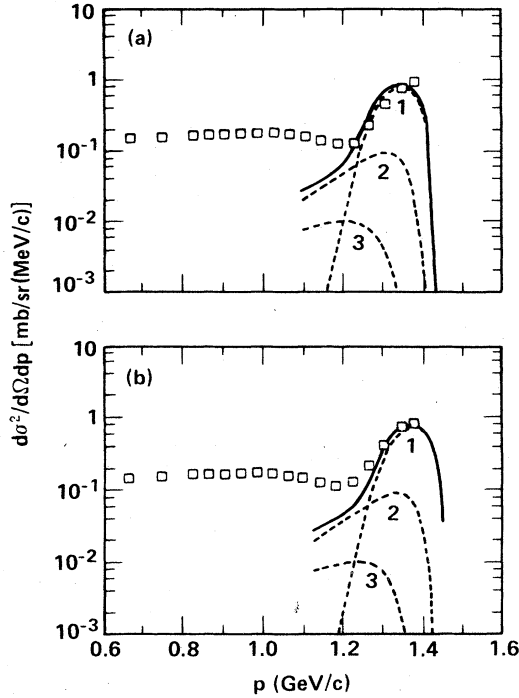


FIG. 2. (a) Quasi-elastic cross section (solid line) at $\theta=15^\circ$ based on Eqs. (51) and (36a) of text. Data are from Refs. 9 and 10. Dotted lines labeled $n=1,2,3$ indicate contributions from single, double, and triple knockout. (b) Same results shifted in energy by $\Delta\omega=\epsilon_B$ as in Eq. (52). All curves in this paper are for 800 MeV protons incident on ^{12}C .

proton momentum in Fig. 2(a) along with the inclusive (p,p') data from Ref. 9. Dotted lines labeled $n=1,2,3$ are contributions from single, double, and triple knockout, and the solid curve is the full quasi-elastic cross section summed through $n=3$. The multiple knockout series converges quickly: successive peaks are down by roughly one order of magnitude. We remark that this supports the use of approximation (23) which eliminated θ functions responsible for z ordering in ground state matrix elements. Because of the scalar distortion, only z ordering of the hard collisions is important, and the lowest order correction to (23), which involves triple scattering terms, now involves only the small triple *knockout* term. The single and double knockout cross sections calculated with scalar distortion are exact in the sense of approximation (23).

The normalization of the quasi-elastic peak in Fig. 2(a) agrees very well with the data, although the peak position is shifted towards larger energy loss. Such a shift has been seen before in PWIA and DWIA calculations.^{4,6} As suggested in Ref. 6, the shift could be due to the neglect of distortion on the unobserved particle. At low scattering angles the momentum transferred to the struck particle is small enough that it may not escape but remain bound in an excited nuclear state. The single particle shell model response functions [(44b) and (45)], which determine the position and width of the peak, would in this case be inadequate both because of the use of plane waves and because the kinematics involve the full binding energy

ϵ_B and the kinetic energy $k_i^2/2m$ of a knocked out particle.

In the present model it is important to account for this shift in some way, because the spin observables are expected to exhibit structure in the kinematic region where the double knockout term dominates. Therefore all cross sections and spin observables will be plotted as a function of a shifted energy transfer:

$$d\sigma(q_\perp, \omega)_{\text{shown}} = d\sigma(q_\perp, \omega - \epsilon_B)_{\text{calculated}}. \quad (52)$$

This does a good job of bringing the quasi-elastic peak in line with the data as seen in Fig. 2(b). The $n=1,2,3$ quasi-elastic cross sections at $\theta=8^\circ, 11^\circ, 15^\circ$, and 20° are shown as dotted lines in Figs. 5(a), (c), (e), and (g). All curves shown in this paper except for Fig. 2(a) are plotted with the shift (52).

A breakdown of numerical accuracy occurs when the cross sections drop $\gtrsim 3$ orders of magnitude below their peak values. In the kinematic region where they were calculated ($0 \leq \omega - \epsilon_B \leq 0.2$ GeV) only the single knockout terms exhibited this breakdown. Therefore, the single knockout S_{ij} 's were extended beyond the region of convergence by assuming they fall off exponentially in ω . This is consistent with the asymptotic form of the single particle response function (45) for fixed q_\perp as $\omega \rightarrow \infty$.

B. Quasi-elastic spin observables

The five independent spin observables D_{nn} , D_{qq} , D_{zz} , D_{qz} , and A_y are shown at $\theta=15^\circ$ in Fig. 3 (solid lines). In order to display the effect of the multiple knockout contributions, the quantities $D_{ij}^{(n)}$ ($n=1,2,3$) are also shown (dotted lines). These are defined by

$$D_{ij}^{(n)} = S_{ij}^{(n)} / S_{00}^{(n)}, \quad (53)$$

$$S_{ij} = \sum_{n=1}^A S_{ij}^{(n)}.$$

The $D_{ij}^{(n)}$'s are what the spin observables would be if only processes involving n knockouts are included. In the region of low energy transfer (high p) $D_{ij} \cong D_{ij}^{(1)}$, but at higher energy loss the double knockout cross sections dominate and $D_{ij} \cong D_{ij}^{(2)}$. In all cases this causes a drop in the spin observables in the double scattering region ($p \lesssim 1.27$ GeV/c at $\theta=15^\circ$).

The effect of distortion on the single knockout terms can be seen by comparing the long dashed lines in Figs. 3(a)–(e) which show the plane wave results $(D_{ij}^{(1)})_{\text{PW}}$ (these are the same as $D_{ij}^{(1)}$ with $\Omega \rightarrow 1$). In the single knockout region ($p \gtrsim 1.27$ GeV/c) the distortion produces only a small deviation from the plane wave results. Figure 3(f) shows the plane wave polarization $(A_y)_{\text{PW}}$ and $(A_y^{(n)})_{\text{PW}}$ ($n=1,2,3$). Comparing Fig. 3(e) we see that the distortion has even less effect on the multiple knockout terms. The distortion provides the same nearly constant normalization term by term in the multiple knockout series. That is

$$S_{ij}^{(n)}(q_\perp, \omega) \cong \mathcal{D}^{(n)}[S_{ij}^{(n)}(q_\perp, \omega)]_{\text{PW}}, \quad (54)$$

and therefore $D_{ij}^{(n)} \cong (D_{ij}^{(n)})_{\text{PW}}$. This normalization varies with n ($\mathcal{D}^{(1)} \sim \frac{1}{4}$ while $\mathcal{D}^{(2)} \sim \frac{1}{8}$), which can slightly

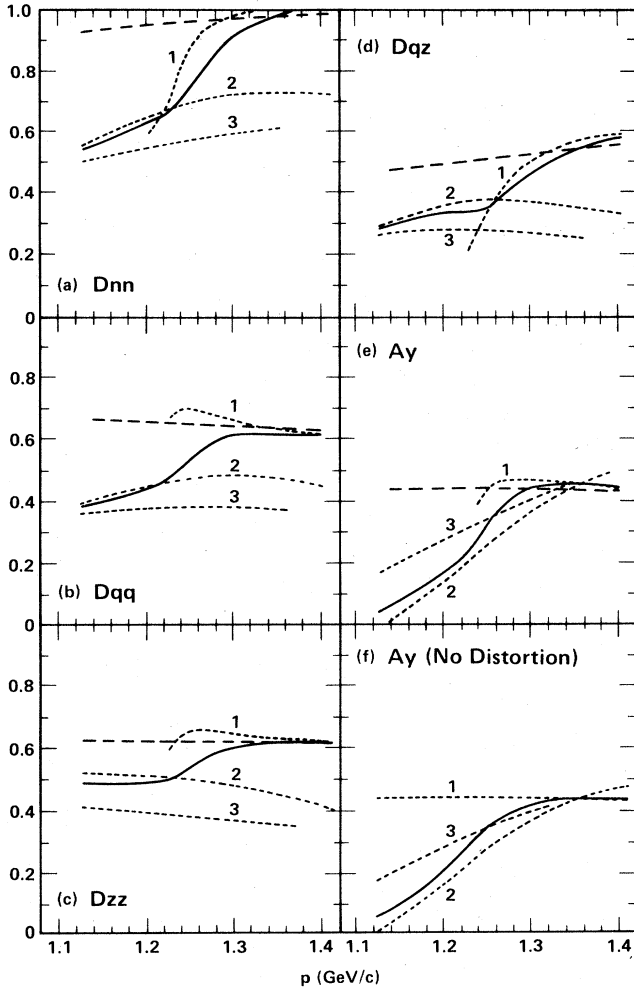


FIG. 3. Quasi-elastic spin observables D_{ij} at $\theta=15^\circ$ (solid lines). Dotted lines labeled $n=1,2,3$ show $D_{ij}^{(n)}$, and the dashed line is $D_{ij}^{(1)}$ with no distortion. (f) shows A_y and $A_y^{(1)}$ ($n=1,2,3$) with no distortion.

change the full D_{ij} compared to $(D_{ij})_{PW}$ because it affects how quickly D_{ij} falls from $D_{ij}^{(1)}$ to $D_{ij}^{(2)}$ when passing from the single to double knockout region. Calculations were also performed by evaluating the distortion factors at the classical impact parameter:

$$\Omega^*(b')\Omega(b) \rightarrow |\Omega(B)|^2, \quad (55)$$

which amounts to forcing all the momentum transfer to occur on the hard collisions [this can be seen by performing the $\int d^2\beta$ integral in (51) using the expression (44a) with (41a) for $\bar{W}_{ij}^{(n)}$; the result is a factor

$$\delta^2 \left[\mathbf{q}_1 - \sum_{i=1}^n \mathbf{Q}^{(i)} \right],$$

where $\mathbf{Q}^{(i)}$ is the momentum transferred on the i th hard collision]. The $D_{ij}^{(n)}$'s computed with the replacement (55) are almost identical to the plane wave results. Thus,

momentum transferred in the elastic collisions participating in the distortion is responsible for the difference between $D_{ij}^{(n)}$ and $(D_{ij}^{(n)})_{PW}$ seen in Fig. 3.

In order to test the assumption of scalar distortion, the single knockout cross section and A_y were calculated with the full spin dependent Ω [Eq. (48)] based on Eq. (28). In addition, all $\nabla\rho_w$ terms which remain in the short range approximation (47) were kept. The spin structure in (28) combined with the presence of these extra terms make this calculation considerably more complicated (see Ref. 15 for details). The results are shown in Fig. 4 at $\theta=15^\circ$. Solid lines are $d^2\sigma^{(1)}/d\Omega dp$ and $A_y^{(1)}$ with scalar distortion, crosses indicate results of the full calculation with all $\nabla\rho_w$ terms, and the dashed line in (b) is $(A_y^{(1)})_{PW}$. We see that the distortion, whether scalar or spin dependent, leaves the polarization largely unchanged from the plane wave result.

Predictions for the laboratory spin observables DNN , DLL , DSS , DLS , and DSL are shown in Figs. 5(b), (d), (f), and (h) along with the calculation and inclusive (p,p') data for A_y .¹⁰ The normalization of A_y is a little off: ~ 0.4 in the single knockout region compared to ~ 0.3 in the data, but the drop from ~ 0.3 to ~ 0.1 is clearly accounted for by the double knockout term. There is further structure in the data, namely the "shoulders" seen most clearly at 11° , 15° in the 1.0 – 1.25 GeV/c range. As suggested in Ref. 10, these are most likely a signature of quasi-free Δ production. The polarization data on inelastic p-p scattering show a corresponding peak in A_y just

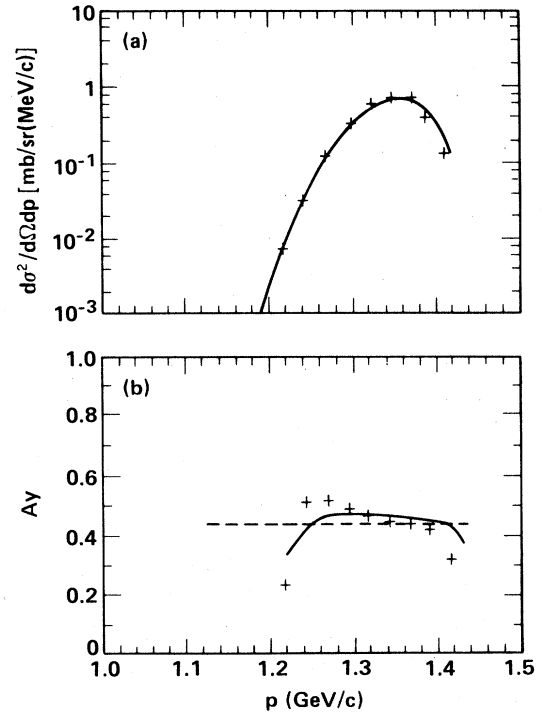


FIG. 4. Single knockout cross section (a) and A_y (b) at $\theta=15^\circ$ with spin-dependent distortion (crosses) and scalar distortion (solid curves). In (b) the long-dashed curve is $A_y^{(1)}$ with no distortion.

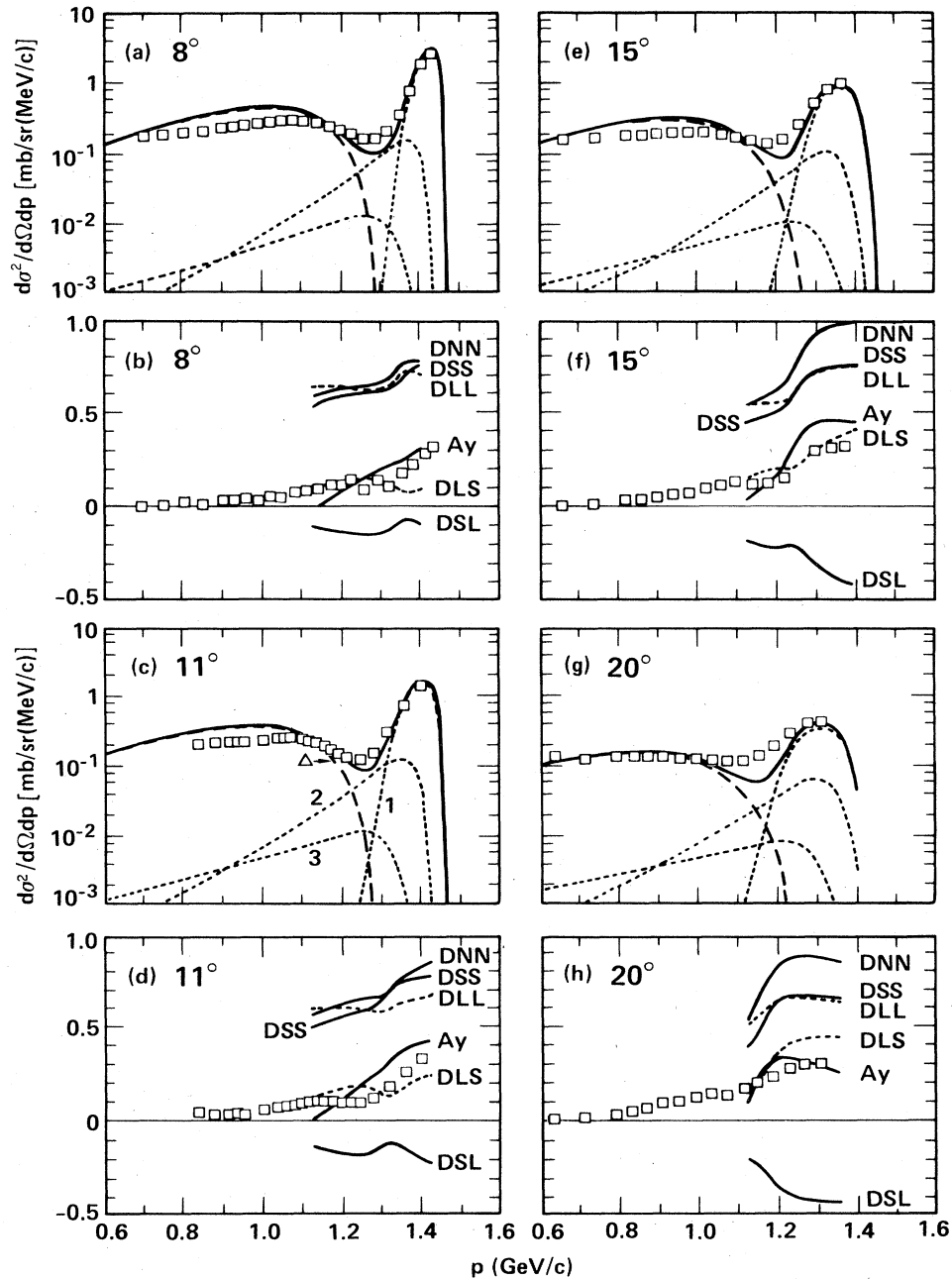


FIG. 5. Cross sections and laboratory spin observables DNN , DLL , DSS , DLS , DSL , and A_y . In (a), (c), (e), and (g) dotted lines are the $n=1,2,3$ quasi-elastic cross sections; the long-dashed line is the Δ production cross section based on Eq. (56) of text, and the solid line is the sum of these. In (b), (d), (f), and (h) DLL and DLS are shown as dotted lines. Also shown are data for the inclusive (p,p') cross sections and A_y from Refs. 9 and 10.

where the inelastic cross section begins to rise (presumably due to the Δ). Evidently this peak is smoothed out in the nucleus and appears as a low shoulder which, as the Δ production begins to dominate the cross section, becomes distinguishable in a background of quasi-elastic scattering. Having isolated the quasi-elastic contribution, it should now be possible when data becomes available to look for similar signatures of quasi-free Δ production in the other spin observables.

C. The Δ region

A single scattering impulse approximation should work well in the Δ region because processes involving the creation of more than one Δ with mass $m_\Delta > m + m_\pi$ are not energetically favorable. Therefore, as a preliminary step in understanding the Δ region, multiple scattering theory has been used to normalize the PWIA calculation of the cross section $d^2\sigma_\pi/d\Omega dp$ for $p + A \rightarrow p + \pi + A^*$

from Ref. 5, which is based on spin-independent $NN \rightarrow NN\pi$ amplitudes calculated in a one-pion exchange model. No attempt will be made to calculate spin observables due to Δ production because the spin dependence of the $NN \rightarrow N\Delta$ and $NN \rightarrow NN\pi$ amplitudes is poorly known and strongly energy dependent.

The normalized PWIA has the form:

$$\frac{d^2\sigma_\pi}{d\Omega dp} = \mathcal{D}_\pi(E_k, E_p) \left(\frac{d^2\sigma_\pi}{d\Omega dp} \right)_{PW} \quad (56)$$

This assumes all momentum and energy transfer occurs on one quasi-free $NN \rightarrow NN\pi$ collision. The distortion factor \mathcal{D}_π depends on the energy of the fast nucleon before and after this collision. To indicate how it is derived, consider the analogy in the quasi-elastic case. As in Eq. (54), suppose

$$\frac{d^2\sigma^{(1)}}{d\Omega dp} = \mathcal{D}^{(1)} \left(\frac{d^2\sigma^{(1)}}{d\Omega dp} \right)_{PW} \quad (57)$$

$\mathcal{D}^{(1)}$ can be derived from Eq. (51) if, in addition to the replacement $\Omega^*(b')\Omega(b) \rightarrow |\Omega(B)|^2$, we also approximate the Wigner transform by

$$\begin{aligned} \tilde{\rho}_w(B, p) &\cong t(B)n(p), \\ t(b) &= \int dz \rho(B, z). \end{aligned} \quad (58)$$

[Both of these approximations were made by KKP; they used the momentum density $n(p) \sim \theta(k_F - p)$.] Now the $\int d^2B$ integral completely separates, and we find

$$\mathcal{D}^{(1)} = \int d^2B t(B) |\Omega(B)|^{2(A-1)}. \quad (59)$$

In the Δ production case, a similar derivation yields (see Ref. 15 for details):

$$\mathcal{D}_\pi(E_k, E_p) = \int d^2B t(B) \frac{1}{A} \sum_{(m+n=A-1)} D_k^m(B) D_p^n(B). \quad (60)$$

Here D_k (D_p) represents the distortion in the initial (final) state due to the elastic or quasi-elastic scattering off a target nucleon at energy E_k (E_p). It is given in the short range approximation by

$$D_p(B) = 1 - \sigma_{in}^{NN}(E_p) t(B). \quad (61)$$

$\sigma_{in}^{NN}(E_p)$ is the inelastic NN cross section for a nucleon at incident energy E_p . \mathcal{D}_π varies from ~ 0.5 at $p=1460$ MeV/c to ~ 0.7 at $p=800$ MeV/c. This behavior arises because at large energy loss E_p drops below threshold and $\sigma_{in}^{NN} \rightarrow 0$ causing $D_p \rightarrow 1$. These values of \mathcal{D}_π are quite different from the normalization of the quasi-elastic peak ($\mathcal{D}^{(1)} \sim \frac{1}{4}$) which contrasts with the procedure used in Ref. 5 where the PWIA calculations of both peaks were normalized to the data by the same factor. (The calculations in Ref. 5 also contained an error. The cross section has two pieces called the "recoil" and "decay" terms which depend, respectively, on whether the Δ is made in the projectile or a target nucleon. The recoil contribution is smaller and has a more narrow peak than the decay cross section which is wider and flatter as a function of

energy transfer. In Ref. 5 the decay cross section was too big by a factor of 4. As a result it washed out the recoil term and the Δ peak appeared broader than it should have. This seemed alright because the data prefers a broader Δ peak, and the factor of ~ 4 error in magnitude was compensated by normalizing both Δ and quasi-elastic peaks with a slowly varying function of θ approximately equal to $\frac{1}{4}$.)

Dashed lines in Figs. 5(a), (c), (e), and (g) show the PWIA production cross section normalized by \mathcal{D}_π as in (56). The solid lines are the sum of this plus the $n=1,2,3$ quasi-elastic contributions, which were extended into the Δ region in these plots by assuming an exponential fall off in ω . The calculation of $(d^2\sigma_\pi/d\Omega dp)_{PW}$ is essentially the same as in Ref. 5 except the $NN \rightarrow NN\pi$ amplitudes were slightly modified to better fit the hydrogen data.¹⁵ The positions of the Δ peaks agree fairly well with the data although they are too high and narrow. Also, the dip region is not filled in enough to meet the data, suggesting both Δ production and quasi-elastic contributions should be larger in this region. The quasi-elastic peaks may be too narrow because the response function (45) depends on q_\perp rather than q due to the eikonal approximation. However, the calculation of $(d^2\sigma_\pi/d\Omega dp)_{PW}$ did not involve an eikonal approximation. The fact that it is too high and narrow suggests the Δ may have a broader width in the nuclear medium. More concrete evidence for such a broadening has been seen in recent inelastic electron-nucleus experiments¹⁹ which show a broader Δ peak in the nuclear data compared to the hydrogen data, even if broadening due to Fermi motion is taken into account.

V. CONCLUSION AND SUMMARY

We have developed a method for calculating spin observables due to quasi-free nucleon knockout in high energy (p,p') reactions. This is based on an extension of Glauber theory to include noncommuting spin-dependent NN interactions and multiple inelastic collisions. Calculations have been performed at 800 MeV on ¹²C for the quasi-elastic cross section $d^2\sigma/d\Omega dp$ and all spin observables consistent with parity conservation: A_y , D_{NN} , D_{LL} , D_{LS} , D_{SS} , and D_{LS} . The distortion due to elastic NN collisions normalizes the cross sections, which agree in magnitude extremely well with the data. The distortion has little effect on the spin observables, however, which are ratios of spin dependent to spin averaged cross sections. In the analysis, certain terms involving the gradient of the nuclear density $\nabla_b \rho(b, z)$ were dropped in order to simplify the spin algebra. A more detailed investigation of the single knockout contribution to $d^2\sigma/d\Omega dp$ and A_y shows that this approximation is justified. In all cases multiple knockout contributions cause a drop in the spin observables in the kinematic region where they dominate the cross section. This explains the drop from ~ 0.3 to ~ 0.1 in the inclusive data for $A_y(\theta, p)$ seen in the dip region between quasi-elastic and Δ production peaks. Further structure in the inclusive A_y data most likely corresponds to quasi-free Δ production. A PWIA calculation

of the single Δ production cross section, normalized using multiple scattering theory, suggests the Δ may have a broader width in the nucleus compared to the free width, agreeing with more conclusive results from electron scattering experiments. Also, in contrast to previous theoretical analyses, multiple scattering theory predicts that the Δ and quasi-elastic cross sections are normalized differently by the distortion (the quasi-elastic PWIA is reduced by $\approx \frac{1}{4}$ while the Δ PWIA is reduced by ~ 0.5 to 0.7). Future PWIA calculations which take into account

a larger Δ width, even if only phenomenologically, may be able to successfully describe both cross sections and spin observables in the Δ region. First, however, more accurate knowledge of the free spin-dependent $NN \rightarrow N\Delta \rightarrow NN\pi$ amplitudes is needed.

This work was performed at the University of Maryland under DOE Contract No. 01-5-27078, and at Lawrence Livermore National Laboratory under DOE Contract No. W-7405-ENG-48.

-
- ¹R. J. Glauber, *Lectures in Theoretical Physics*, edited by W. E. Britten and L. G. Dunham (Interscience, New York, 1959), Vol. I, p. 315.
- ²A. Kerman, H. McManus, and R. Thaler, *Ann. Phys. (N.Y.)* **8**, 551 (1959).
- ³J. A. McNeil, J. R. Shepard, and S. J. Wallace, *Phys. Rev. Lett.* **50**, 1439 (1983).
- ⁴F. R. Kroll and N. S. Wall, *Phys. Rev. C* **1**, 138 (1970).
- ⁵Y. Alexander, J. W. Van Orden, E. F. Redish, and S. J. Wallace, *Phys. Rev. Lett.* **44**, 1579 (1980).
- ⁶R. E. Chrien *et al.*, *Phys. Rev. C* **21**, 1014 (1980).
- ⁷H. Krimm, A. Klar, and H. J. Pirner, *Nucl. Phys.* **A367**, 333 (1981).
- ⁸M. Thies, *Ann. Phys. (N.Y.)* **123**, 411 (1979).
- ⁹J. A. McGill *et al.*, *Phys. Rev. C* **29**, 204 (1984).
- ¹⁰J. A. McGill *et al.*, *Phys. Lett.* **134B**, 157 (1984). (Previously unpublished data at 8° used with permission of J. A. McGill.)
- ¹¹K. M. Watson, *Phys. Rev.* **89**, 575 (1953); M. Goldberger and K. M. Watson, *Collision Theory* (Wiley, New York, 1964).
- ¹²S. J. Wallace, *High Energy Proton Scattering*, *Advances in Nuclear Physics*, Vol. 12, edited by J. W. Negele and E. Vogt (Plenum, New York, 1981).
- ¹³V. Mandelsweig and S. J. Wallace, *Phys. Rev. C* **25**, 61 (1981).
- ¹⁴R. A. Arndt *et al.*, *Phys. Rev. D* **28**, 97 (1983).
- ¹⁵Richard D. Smith, Ph.D. dissertation, University of Maryland, 1984 (unpublished).
- ¹⁶J. M. Moss, *Phys. Rev. C* **26**, 727 (1982).
- ¹⁷R. J. Glauber and G. Matthiae, *Nucl. Phys.* **B21**, 135 (1970); P. Osland and R. J. Glauber, *ibid.* **A326**, 255 (1979).
- ¹⁸Y. Horikawa, F. Lenz, and N. C. Mukhopadhyay, *Phys. Rev. C* **22**, 1680 (1980).
- ¹⁹J. S. O'Connell *et al.*, *Phys. Rev. Lett.* **53**, 1627 (1984).